https://doi.org/10.31489/2025M2/208-221 *Research article*

Non-polynomial spline method for singularly perturbed differential difference equations with delay and advance terms

A.M. Regal, S.D. Kumar*

School of Advanced Sciences, Vellore Institute of Technology, Vellore, India
(E-mail: akhilamariyard@gmail.com, mathdinesh005@gmail.com)

In this study, we introduced a non-polynomial spline technique to address singularly perturbed differential difference equations involving both delay and advanced parameters. This method exhibits a linear rate of convergence, and we have thoroughly analyzed its convergence properties. To demonstrate the effectiveness of this approach, we provided two numerical examples. We presented the maximum absolute errors in tabular form and displayed the pointwise absolute errors using graphical representations. Additionally, we included tables showing the numerically obtained rate of convergence.

Keywords: singular perturbation problems, numerical methods, delay parameter, advanced parameter, non-polynomial spline.

2020 Mathematics Subject Classification: 65L06, 65L11, 65L20, 65L50.

Introduction

Singularly perturbed problems are a class of differential equations characterized by the presence of a small parameter, which causes the solutions to exhibit rapid changes over small regions of the domain. When these problems incorporate delay (time-lagged terms) and advanced (time-advanced terms) parameters, they form a more complex subclass of differential equations that present unique challenges and opportunities for both theoretical and applied mathematics. The importance of singularly perturbed problems with delay and advanced parameters stems from their ability to model real-world phenomena where current states are influenced by past and future states. They capture dynamics occurring at multiple temporal or spatial scales, providing a more comprehensive understanding of the systems. The inclusion of delay and advanced terms models systems where interactions are not instantaneous but depend on previous or future states, reflecting more realistic scenarios. Also, they allow for the study of stability and transitions in systems. The scope of singularly perturbed problems with delay and advanced parameters is broad and interdisciplinary, encompassing mathematical theory, control theory, biological systems, engineering and so on. The design of robust control algorithms for systems with feedback delays and modeling data flow and congestion where delays are inherent are done in engineering systems. Their applications in biological and medical sciences include epidemiology, neural dynamics etc. These equations play a vital role in economics and finance for market dynamics and supply chains. Climate models and ecological systems can also be studied using these equations. Singularly perturbed problems with delay and advanced parameters are crucial for accurately modeling and analyzing systems where time-dependent interactions play a significant role. Their importance spans various fields, including engineering, biology, economics, and environmental science. The scope of these problems is vast, involving complex mathematical techniques and interdisciplinary applications, making them a significant area of study in both theoretical and applied research. These problems offer a powerful framework for understanding and designing future systems with intricate dynamics

*Corresponding author. *E-mail: mathdinesh005@gmail.com*
Received: 13 June 2024; *Accepted:* 22 January 2025.

and time-dependent interactions. Their ability to capture delays, advancements, and rapid transitions makes them invaluable tools for various scientific and technological advancements. Understanding and solving these problems provide deeper insights into the behavior of complex systems, offering robust solutions to real-world challenges.

Numerous researchers have delved into the realm of singularly perturbed small delayed problems of reaction diffusion type. A fourth order exponentially fitted numerical scheme is used in [1] to find the solution of the aforementioned problem. The works in [2] and [3] have also dealt with these problems. Trigonometric cubic B-spline function is utilized in [4] and then the matrix system obtained is solved using Thomas Algorithm. The authors in [5] used non-polynomial spline approach to solve SPDDEs of reaction- diffusion type, whereas a new approach is done in [6] for these type of problems. Furthermore, research has been conducted on convection diffusion type problems as well. Some others concentrated on singularly perturbed large delay differential equations and the systems of these problems. Cubic spline in tension scheme is used in [7] to solve SPDDEs with large delay, whereas the authors in [8] used non-polynomial spline approach to solve them. Convection diffusion type problems under this category is worked in [9] and the researchers in [10] approximated these problems involving integral as end boundary condition by exploring compression technique. SPDDEs of reaction diffusion type with large delay is also addressed by the researchers [11–13]. Non-polynomial spline technique is used [14] to deal with the system of SPDDEs with large delay. The studies in [15] and [16] also concentrated on system of SPDDEs with different techniques. Also, few studies have been done in the area of singularly perturbed delay differential equations involving delay and advanced parameters in the interval $(0, 1)$. They considered the SPDDE with small negative and positive shifts. The authors in [17] used mixed finite difference method via domain decomposition and [18] used numerical integration technique to handle these problems. A meshless approach is explored in [19] to arrive at the numerical approximation of the problem and they have used multiquadric radial basis functions collocation method, which is then coupled with residual subsampling algorithm for support adaptivity. A successive complementary expansion method is used by the researchers in [20]. Many other methods [21–23] have explored SPDDEs with small mixed shifts.

Here, we are considering the problem with large shifts, that is, we consider the following singular perturbation problem involving delay and advanced parameters:

$$\mathcal{H}\kappa \equiv -\xi\kappa''(x) + p(\eta)\kappa'(x) + q(x)\kappa(x) + r(x)\kappa(x-1) + s(x)\kappa(x+1) = t(x),\ x \in \omega = (0,3), \tag{1}$$

satisfying

$$\begin{array}{rcll} \kappa(x) & = & u(x), & x \in [-1,0], \\ \kappa(x) & = & v(x), & x \in [3,4], \end{array} \tag{2}$$

where $0 < \xi \leq 1$ and u, v are functions defined on $[-1, 0]$ and $[3, 4]$ respectively. It is assumed that $p(x) \geq \bar{p} \geq \bar{\bar{p}} > 0$, $q(x) \geq \bar{q} \geq 0$, $\bar{r} \leq r(x) \leq 0$, $s(x) \geq \bar{s} \geq 0$, $\bar{q} + \bar{r} \geq \bar{\beta} > 0$ and the coefficients are smooth functions on $\bar{\gamma}$.

1 Analytical Results

Equations (1) and (2) can be written as:

$$\mathcal{H}\kappa \equiv \mathcal{F}(x),$$

where

$$\mathcal{H}\kappa = \begin{cases} \mathcal{H}_1\kappa(x) & = & -\xi\kappa''(x) + p(x)\kappa'(x) + q(x)\kappa(x) + s(x)\kappa(x+1), & x \in (0,1], \\ \mathcal{H}_2\kappa(x) & = & -\xi\kappa''(x) + p(x)\kappa'(x) + q(x)\kappa(x) + r(x)\kappa(x-1) + s(x)\kappa(x+1), & x \in (1,2], \\ \mathcal{H}_3\kappa(x) & = & -\xi\kappa''(x) + p(x)\kappa'(x) + q(x)\kappa(x) + r(x)\kappa(x-1), & x \in (2,3], \end{cases}$$

$$\mathcal{F}(x) = \begin{cases} t(x) - r(x)\kappa(x-1), & x \in (0,1], \\ t(x), & x \in (1,2], \\ t(x) - s(x)\kappa(x+1), & x \in (2,3], \end{cases}$$

with boundary conditions,

$$\kappa(1^-) = \kappa(1^+),\ \kappa'(1^-) = \kappa'(1^+),\ \kappa(x) = u(x),\ x \in [-1,0],$$
$$\kappa(2^-) = \kappa(2^+),\ \kappa'(2^-) = \kappa'(2^+),\ \kappa(x) = v(x),\ x \in [3,4].$$

Throughout the work, we take $\gamma = (0,3)$, $\bar{\gamma} = [0,3]$, $\gamma_1 = (0,1)$, $\gamma_2 = (1,2)$, $\gamma_3 = (2,3)$, $\gamma^* = \gamma_1 \cup \gamma_2 \cup \gamma_3$ and $\varpi = C^0(\bar{\gamma}) \cap C^1(\gamma) \cap C^2(\gamma^*)$.

Lemma 1. Let $\omega(x)$ be any function in $C^0(\bar{\gamma}) \cap C^1(\gamma) \cap C^2(\gamma^*)$ such that $\omega(0) \geq 0$, $\omega(3) \geq 0$, $\mathcal{H}_1\omega(x) \geq 0$, for all $x \in \gamma_1$, $\mathcal{H}_2\omega(x) \geq 0$, for all $x \in \gamma_2$, $\mathcal{H}_3\omega(x) \geq 0$, for all $x \in \gamma_3$, $[\omega']1) \leq 0$ and $[\omega']2) \leq 0$, then $\omega(x) \geq 0$, $\forall x \in \bar{\gamma}$.

Proof. Define the function $a(x)$ as

$$a(x) = \begin{cases} \frac{1+3x}{12}, & x \in [0,1], \\ \frac{1+x}{6}, & x \in [1,2], \\ \frac{4+x}{12}, & x \in [2,3]. \end{cases}$$

It is clear that $a(x)$ is positive for all x in $\bar{\gamma}$. Also note that $\mathcal{H}a(x) > 0$ for all $x \in \gamma^*$; $a(0)$ and $a(3)$ are strictly positive and $[a]'(1)$ and $[a]'(2)$ are less than zero. Consider the set $\left\{\frac{-\omega(x)}{a(x)}\right\}$ and let its maximum be denoted by M in $\bar{\gamma}$. Then $\exists x_0 \in \bar{\gamma}$ satisfying $\omega(x_0) + Ma(x_0) = 0$ and $\omega(x_0) + Ma(x_0) \geq 0$ for all $x \in \bar{\gamma}$. This implies that $(\omega + Ma)(x_0)$ gives minimum value.

If $M < 0$, then $\omega(x) \geq 0$. If $M > 0$, then the function $a(x)$ to be non-negative is not possible. We consider the following cases to prove the same.

Case (a): $x_0 = 0$.

Then,

$$0 < (\omega + Ma)(0) = \omega(0) + Ma(0) = 0,$$

which is a contradiction.

Case (b): $x_0 \in \gamma_1$.

Then,

$$0 < \mathcal{H}_1(\omega + Ma)(x_0) = -\xi(\omega + Ma)''(x_0) + p(x_0)(\omega + Ma)'(x_0) + q(x_0)(\omega + Ma)(x_0) + s(x_0)(\omega + Ma)(x_0 + 1) \leq 0,$$

which is a contradiction.

Case (c): $x_0 = 1$.

Then,

$$0 \leq [(\omega + Ma)'](1) = [\omega'](1) + M[a'](1) < 0,$$

it is a contradiction.

Case (d): $x_0 \in \gamma_2$.

Then,

$$0 < \mathcal{H}_2(\omega + Ma)(x_0) = -\xi(\omega + Ma)''(x_0) + p(x_0)(\omega + Ma)'(x_0) + q(x_0)(\omega + Ma)(x_0) + r(x_0)(\omega + Ma)(x_0 - 1) + s(x)(\omega + Ma)(x_0 + 1) \leq 0,$$

it is again a contradiction.

Case (e): $x_0 = 2$.
Then,

$$0 \leq [(\omega + Ma)']'](2) = [\omega']'](2) + M[a']'](2) < 0,$$

which is a contradiction.
Case (f): $x_0 \in \gamma_3$.
Then,

$$0 < \mathcal{H}_3(\omega + Ma)(x_0) = -\xi(\omega + Ma)''(x_0) + p(x_0)(\omega + Ma)'(x_0) + q(x_0)(\omega + Ma)(x_0) + r(x_0)(\omega + Ma)(x_0 - 1) \leq 0,$$

which is a contradiction.
Case (g): $x_0 = 3$.
Then,

$$0 \leq [(\omega + Ma)](3) = \omega(3) + Ma(3) = 0,$$

which is again a contradiction.
By considering all the above cases, the proof is complete.

Lemma 2. The solution $\kappa(x)$ for the problem (1)–(2) satisfies the bound:

$$\mid \kappa(x) \mid \leq \bar{C} \max\{\sup_{r \in \gamma^*} \mid \mathcal{H}\kappa(x) \mid, \mid \kappa(0) \mid, \mid \kappa(3) \mid\}, \quad x \in \bar{\bar{\gamma}}.$$

Proof. Let us define two new functions, denoted by ϑ^+ and ϑ^-. They are defined as:

$$\vartheta^{\pm}(x) = \bar{C}\bar{M}a(x) \pm \kappa(x), \ x \in \bar{\gamma},$$

where $\bar{M}$ denotes the maximum of the set $\{\sup_{r \in \gamma^*} \mid \mathcal{H}\kappa(x) \mid, \mid \kappa(0) \mid, \mid \kappa(3) \mid\}$ and $a(x)$ is the function in the above lemma. By using these newly defined functions within the previously mentioned lemma, we will get the desired result.

Lemma 3. Let $\kappa(x)$ be the solution for the problem (1)–(2). Then

$$\|\kappa^{(k)}(x)\|_{\gamma^*} \leq C\xi^{-k}, \text{ for } k = 1, 2, 3, 4.$$

Proof. First, we prove that $\kappa'(x)$ is bounded on ω_1. Consider $\mathcal{H}_1(x)$ and integrate its both sides, then

$$\begin{aligned} -\xi(\kappa'(x) - \kappa'(0)) &= -[p(x)\kappa(x) - p(0)\kappa(0)] + \int_0^x p'(x)\kappa(x)dx - \int_0^x q(x)\kappa(x)dx \\ &\quad - \int_0^x s(x)\kappa(x+1)dx + \int_0^x (t(x) - r(x))u(x-1)dx, \\ \xi\kappa'(0) &= \xi\kappa'(x) - [p(x)\kappa(x) - p(0)\kappa(0)] + \int_0^x p'(x)\kappa(x)dx - \int_0^x q(x)\kappa(x)dx \\ &\quad - \int_0^x s(x)\kappa(x+1)dx + \int_0^x (t(x) - r(x))u(x-1)dx. \end{aligned}$$

Using mean value theorem, we get $\mid \xi\kappa'(x) \mid \leq C(\mid\mid \kappa(x) \mid\mid, \mid\mid t(x) \mid\mid, \mid\mid u \mid\mid_{[-1,0]})$, for some x in $(0, \xi)$ and $\mid \kappa'(0) \mid \leq C(\mid\mid \kappa(x) \mid\mid + \mid\mid t(x) \mid\mid + \mid\mid u(x) \mid\mid)$. Hence, we have $\mid \kappa'(x) \mid \leq C \max\{\mid\mid \kappa(x) \mid\mid, \mid\mid t(x) \mid\mid, \mid\mid u \mid\mid\}$, x in ω_1.

Now consider $\mathcal{H}_2(x)$ and integrate its both sides, then

$$\begin{aligned}
-\xi(\kappa'(x)-\kappa'(0)) &= -[p(x)\kappa(x)-p(0)\kappa(0)]+\int_0^x p'(x)\kappa(x)dx-\int_0^x q(x)\kappa(x)dx \\
&\quad -\int_0^x r(x)\kappa(x-1)dx-\int_0^x s(x)\kappa(x+1)dx+\int_0^x t(x)dx, \\
\xi\kappa'(0) &= \xi\kappa'(x)-[p(x)\kappa(x)-p(0)\kappa(0)]+\int_0^x p'(x)\kappa(x)dx-\int_0^x q(x)\kappa(x)dx \\
&\quad -\int_0^x r(x)\kappa(x-1)dx-\int_0^x s(x)\kappa(x+1)dx+\int_0^x t(x)dx.
\end{aligned}$$

Using mean value theorem, we get $\mid \xi\kappa'(x) \mid \leq C(\mid\mid \kappa(x) \mid\mid, \mid\mid t(x) \mid\mid, \mid\mid u \mid\mid_{[-1,0]})$, for some x in $(0,\xi)$ and $\mid \kappa'(0) \mid \leq C(\mid\mid \kappa(x) \mid\mid + \mid\mid t(x) \mid\mid + \mid\mid u(x) \mid\mid)$. Hence, we have $\mid \kappa'(x) \mid \leq C \max\{\mid\mid \kappa(x) \mid\mid, \mid\mid t(x) \mid\mid, \mid\mid u \mid\mid\}$, x in ω_2.

Now consider $\mathcal{H}_3(x)$ and integrate its both sides, then

$$\begin{aligned}
-\xi(\kappa'(x)-\kappa'(0)) &= -[p(x)\kappa(x)-p(0)\kappa(0)]+\int_0^x p'(x)\kappa(x)dx-\int_0^x q(x)\kappa(x)dx \\
&\quad -\int_0^x r(x)\kappa(x-1)dx+\int_0^x (t(x)-s(x)v(x+1))dx \\
\xi\kappa'(0) &= \xi\kappa'(x)-[p(x)\kappa(x)-p(0)\kappa(0)]+\int_0^x p'(x)\kappa(x)dx-\int_0^x q(x)\kappa(x)dx \\
&\quad -\int_0^x r(x)\kappa(x-1)dx+\int_0^x (t(x)-s(x)v(x+1))dx.
\end{aligned}$$

Using mean value theorem, we get $\mid \xi\kappa'(x) \mid \leq C(\mid\mid \kappa(x) \mid\mid, \mid\mid t(x) \mid\mid, \mid\mid u \mid\mid_{[-1,0]})$, for some x in $(0,\xi)$ and $\mid \kappa'(0) \mid \leq C(\mid\mid \kappa(x) \mid\mid + \mid\mid t(x) \mid\mid + \mid\mid u(x) \mid\mid)$. Hence, we have $\mid \kappa'(x) \mid \leq C \max\{\mid\mid \kappa(x) \mid\mid, \mid\mid t(x) \mid\mid, \mid\mid u \mid\mid\}$, x in ω_3.

Similarly, we can prove for $k = 2, 3, 4$. Hence $\|\kappa^{(k)}(x)\|_{\gamma^*} \leq C\xi^{-k}$, for $k = 1, 2, 3, 4$.

2 Non-Polynomial Spline Approach

Divide the interval $[0, 3]$ into $3N$ mesh intervals with $x_0 = 0$, $x_N = 1$, $x_{2N} = 2$ and $x_{3N} = 3$.

The non-polynomial spline [5] for each interval $[x_i, x_{i+1}]$ has the following form:

$$\begin{aligned}
S_{np}(x) = j_i \sin\alpha(x-x_i) + k_i \cos\alpha(x-x_i) + l_i(\exp(\alpha(x-x_i)) - \exp(-\alpha(x-x_i))) \\
+ m_i(\exp(\alpha(x-x_i)) + \exp(-\alpha(x-x_i))),
\end{aligned}$$

where j_i, k_i, l_i, m_i are the unknown quantities and $\alpha \neq 0$ is the parameter which is used to increase the accuracy of the scheme. From (1), we can write as:

$$\xi\kappa''(x) = p(\eta)\kappa'(x) + q(x)\kappa(x) + r(x)\kappa(x-1) + s(x)\kappa(x+1) - t(x).$$

At $x = x_i$, let $\kappa(x_i) = \kappa_i$, $p(x_i) = p_i$, $q(x_i) = q_i$, $s(x_i) = s_i$, $t(x_i) = t_i$. Then equation (3) becomes

$$\xi\kappa_i'' = p_i\kappa_i' + q_i\kappa_i + r_i\kappa(x_i-1) + s_i\kappa(x_i+1) - t_i.$$

Now, we find the unknowns j_i, k_i, l_i, m_i with the help of following conditions:

$$S_{np}(x_i) = \kappa_i,\ S_{np}(x_{i+1}) = \kappa_{i+1},\ S_{np}''(x_i) = \mathcal{I}_i,\ S_{np}''(x_{i+1}) = \mathcal{I}_{i+1}.$$

Finally, we obtain

$$\begin{array}{ll} j_i = \frac{\kappa_{i+1}\alpha^2 - \mathcal{I}_{i+1} + \cos\beta(\mathcal{I}_i - \alpha^2\kappa_i)}{2\alpha^2 \sin\beta}, & k_i = \frac{-\mathcal{I}_i + \alpha^2\kappa_i}{2\alpha^2}, \\ l_i = \frac{2\alpha^2\kappa_{i+1} + 2\mathcal{I}_{i+1} - (e^{\beta} + e^{-\beta}(\mathcal{I}_i + \alpha^2\kappa_i)}{4\alpha^2(e^{\beta} - e^{-\beta})}, & m_i = \frac{\mathcal{I}_i + \alpha^2\kappa_i}{4\alpha^2}, \end{array} \tag{3}$$

where β is given by αh. Now, we use the following continuity condition: $S'_{np-1}(x_i) = S'_{np}(x_i)$ to get

$$j_{i-1}\cos\beta + k_{i-1}\sin\beta + l_{i-1}(e^{\beta} - e^{-\beta}) + m_{i-1}(e^{\beta} + e^{-\beta}) = j_i + 2l_i.$$

Substituting the values of $j_{i-1}, k_{i-1}, l_{i-1}$ and m_{i-1} using (3) in the above equation, we obtain

$$\begin{aligned} \left(\frac{-\csc\beta}{2} - \frac{1}{e^{\beta} - e^{-\beta}}\right)\kappa_{i-1} + \left(\tan\beta + \frac{e^{\beta} + e^{-\beta}}{e^{\beta} - e^{-\beta}}\right)\kappa_i \\ + \left(\frac{-\csc\beta}{2} - \frac{1}{e^{\beta} - e^{-\beta}}\right)\kappa_{i+1} = \left(\frac{-h^2\csc\beta}{2\beta^2} - \frac{h^2}{(e^{\beta} - e^{-\beta})\beta^2}\right)\mathcal{I}_{i-1} \\ + \left(\frac{h^2\tan\beta}{\beta^2} + \frac{h^2(e^{\beta} + e^{-\beta})}{\beta^2(e^{\beta} - e^{-\beta})}\right)\mathcal{I}_i + \left(\frac{-h^2\csc\beta}{2\beta^2} - \frac{h^2}{(e^{\beta} - e^{-\beta})\beta^2}\right)\mathcal{I}_{i+1}. \end{aligned} \tag{4}$$

Equation (4) can be finally written as:

$$\kappa_{i-1} + \theta_1\kappa_i + \kappa_{i+1} = h^2(\theta_2\mathcal{I}_{i-1} + \theta_3\mathcal{I}_i + \theta_2\mathcal{I}_{i+1}), \tag{5}$$

where

$$\begin{aligned} \theta_1 &= \frac{-2e^{\beta}(\cos\beta + \sin\beta) - 2e^{-\beta}(\sin\beta - \cos\beta)}{e^{\beta} - e^{-\beta} + 2\sin(\beta)}, \\ \theta_2 &= \frac{e^{\beta} - e^{-\beta} - 2\sin\beta}{\beta^2(e^{\beta} - e^{-\beta} + 2\sin\beta)}, \\ \theta_3 &= \frac{-2e^{\beta}(\cos\beta - \sin\beta) + 2e^{-\beta}(\sin\beta + \cos\beta)}{\beta^2(e^{\beta} - e^{-\beta} + 2\sin(\beta))}. \end{aligned}$$

Note that β tends to zero as h approaches zero. As a result, θ_1 tends to -2, θ_2 tends to $\frac{1}{6}$, θ_3 tends to $\frac{2}{3}$. Also, we write $\mathcal{I}_{i-1}$, $\mathcal{I}_i$ and $\mathcal{I}_{i+1}$ as follows:

$$\begin{array}{rcl} \mathcal{I}_{i-1} = \mathcal{I}(x_{i-1}) & = & \frac{1}{\xi}\left(p_{i-1}\kappa'_{i-1} + q_{i-1}\kappa_{i-1} + r_{i-1}\kappa(x_{i-1} - 1) + s_{i-1}\kappa(x_{i-1} + 1) - t_{i-1}\right), \\ \mathcal{I}_i = \mathcal{I}(x_i) & = & \frac{1}{\xi}\left(p_i\kappa'_i + q_i\kappa_i + r_i\kappa(x_i - 1) + s_i\kappa(x_i + 1) - t_i\right), \\ \mathcal{I}_{i+1} = \mathcal{I}(x_{i+1}) & = & \frac{1}{\xi}\left(p_{i+1}\kappa'_{i+1} + q_{i+1}\kappa_{i+1} + r_{i+1}\kappa(x_{i+1} - 1) + s_{i+1}\kappa(x_{i+1} + 1) - t_{i+1}\right). \end{array} \tag{6}$$

We make use of equations in (6) in equation (5) to obtain:

$$\begin{aligned} \xi\left(\kappa_{i-1} + \theta_1\kappa_i + \kappa_{i+1}\right) = h^2\big[\theta_2\left(p_{i-1}\kappa'_{i-1} + q_{i-1}\kappa_{i-1} + r_{i-1}\kappa(x_{i-1} - 1) + s_{i-1}\kappa(x_{i-1} + 1) - t_{i-1}\right) \\ + \theta_3\left(p_i\kappa'_i + q_i\kappa_i + r_i\kappa(x_i - 1) + s_i\kappa(x_i + 1) - t_i\right) \\ + \theta_2\left(p_{i+1}\kappa'_{i+1} + q_{i+1}\kappa_{i+1} + r_{i+1}\kappa(x_{i+1} - 1) + s_{i+1}\kappa(x_{i+1} + 1) - t_{i+1}\right)\big]. \end{aligned}$$

We make use of the following Taylor series approximations for κ'_i, κ'_{i-1} and κ'_{i+1}:

$$\kappa'_i \simeq \frac{\kappa_{i+1} - \kappa_{i-1}}{2h}, \quad \kappa'_{i-1} \simeq \frac{-\kappa_{i+1} + 4\kappa_i - 3\kappa_{i-1}}{2h}, \quad \kappa'_{i+1} \simeq \frac{3\kappa_{i+1} - 4\kappa_i + \kappa_{i-1}}{2h}.$$

Finally, we arrive at the following system of equations:

$$\left(\xi+\frac{3h\theta_2p_{i-1}}{2}-h^2\theta_2q_{i-1}+\frac{h\theta_3p_i}{2}-\frac{h\theta_3p_{i+1}}{2}\right)\kappa_{i-1}+\left(\xi\alpha-2h\theta_2p_{i-1}-h^2\theta_3q_i+2h\theta_2p_{i+1}\right)\kappa_i$$
$$+\left(\xi+\frac{h\theta_2p_{i-1}}{2}-h^2\theta_2q_{i+1}-\frac{h\theta_3p_i}{2}-\frac{3h\theta_2p_{i+1}}{2}\right)\kappa_{i+1}+\left(-h^2\theta_2r_{i-1}\right)\kappa_{i-1-N}+\left(-h^2\theta_3r_i\right)\kappa_{i-N}$$
$$+\left(-h^2\theta_2r_{i+1}\right)\kappa_{i+1-N}+\left(-h^2\theta_2s_{i-1}\right)\kappa_{i-1+N}+\left(-h^2\theta_3s_i\right)\kappa_{i+N}+\left(-h^2\theta_2s_{i+1}\right)\kappa_{i+1+N}$$
$$=-h^2\left(\theta_2t_{i-1}+\theta_3t_i+\theta_2t_{i+1}\right),\ i=1(1)3N-1.$$

We may assume that the coefficients are locally constant because we are examining the differential equations on suitably small subintervals. By applying the Taylor series expansion for $p(x), q(x)$ about the point $x=0$ by restricting to their first terms and from the theory of singular perturbation, an approximation for the solution of the homogeneous problem (1) is of the form

$$\kappa(x)=\kappa_0(x)+\frac{p(0)}{p(x)}\left(\beta-\kappa_0(0)\right)e^{-\left(\frac{p(0)}{\xi}-\frac{q(0)}{p(0)}\right)x}+O(\xi), \tag{7}$$

where $\kappa_0(x)$ is the solution of the reduced problem. Taking the limit as $h\to 0$ in (7) and putting $\rho=\frac{h}{\xi}$, we get

$$\begin{aligned}\lim_{h\to0}\kappa(ih-h) &= \kappa_0(0)+\left(\beta-\kappa_0(0)\right)e^{-(\delta(i-1)\rho)},\\ \lim_{h\to0}\kappa(ih) &= \kappa_0(0)+\left(\beta-\kappa_0(0)\right)e^{-(\delta i\rho)},\\ \lim_{h\to0}\kappa(ih+h) &= \kappa_0(0)+\left(\beta-\kappa_0(0)\right)e^{-(\delta(i+1)\rho)}.\end{aligned}$$

Substituting these limiting values in the obtained scheme, we get the fitting parameter $\sigma=\frac{\rho p_i}{2}\coth(\frac{\rho\delta}{2})$, where $\rho=\frac{h}{\xi}$ and $\delta=\frac{p(0)^2-q(0)\xi}{p(0)}$. Incorporating this fitting factor in the above scheme, we obtain:

$$\bar{E}_i\kappa_{i-1}+\bar{F}_i\kappa_i+\bar{G}_i\kappa_{i+1}+\bar{A}_i\kappa_{i-1-N}+\bar{B}_i\kappa_{i-N}+\bar{C}_i\kappa_{i+1-N}+\bar{H}_i\kappa_{i-1+N}+\bar{I}_i\kappa_{i+N}+\bar{J}_i\kappa_{i+1+N}=\bar{D}_i, \tag{8}$$

where

$$\begin{aligned}\bar{E}_i &= \xi\sigma+\frac{3h\theta_2p_{i-1}}{2}-h^2\theta_2q_{i-1}+\frac{h\theta_3p_i}{2}-\frac{h\theta_2p_{i+1}}{2},\\ \bar{F}_i &= \xi\theta_1\sigma-2h\theta_2p_{i-1}-h^2\theta_3q_i+2h\theta_2p_{i+1},\\ \bar{G}_i &= \xi\sigma+\frac{h\theta_2p_{i-1}}{2}-h^2\theta_2q_{i+1}-\frac{h\theta_3p_i}{2}-\frac{3h\theta_2p_{i+1}}{2},\\ \bar{D}_i &= -h^2\left(\theta_2t_{i-1}+\theta_3t_i+\theta_2t_{i+1}\right),\end{aligned}$$

$$\begin{aligned}\bar{A}_i &= -h^2\theta_2r_{i-1},\quad \bar{B}_i = -h^2\theta_3r_i,\quad \bar{C}_i = -h^2\theta_2r_{i+1},\\ \bar{H}_i &= -h^2\theta_2s_{i-1},\quad \bar{I}_i = -h^2\theta_3s_i,\quad \bar{J}_i = -h^2\theta_2s_{i+1}.\end{aligned}$$

3 Convergence Analysis

The scheme in (8) can be written in matrix form as:

$$T^*U=V, \tag{9}$$

where $T^*=(t_{ij})$ is a $(3N-1\times 3N-1)$ matrix.

Truncation error obtained is $W_i(h) = \frac{h^3}{24}X^* + O(h^4)$, where X^* is given by $\left[\frac{p_{i-1}q_i\kappa_i^{(3)}}{3} + \frac{p_{i+1}\kappa_i^{(3)}}{3} - \frac{10p_i\kappa_i^{(3)}}{6} + \frac{hp_ip_{i+1}\kappa_i^{(3)}}{6} + \frac{hp_ip_{i-1}\kappa_i^{(3)}}{6}\right]$. $T^*U = V$ can also be written as:

$$T^*\overline{U} - W(h) = V, \tag{10}$$

in error form, where $\overline{U} = \begin{pmatrix}\overline{u}_1 & \overline{u}_2 & . & . & . & \overline{u}_{3N-1}\end{pmatrix}^t$ and $W(h) = \begin{pmatrix}w_1 & w_2 & . & . & . & w_{3N-1}\end{pmatrix}^t$ denote the exact solution and truncation error respectively. Let

$$\overline{E}_r = \overline{U} - U = \begin{pmatrix}\bar{e}_1 & \bar{e}_2 & . & . & . & \bar{e}_{3N-1}\end{pmatrix}^t$$

denote the error obtained by numerical approximation. Equations (9) and (10) give

$$T^*\overline{E}_r = W(h). \tag{11}$$

Let $\bar{S}_i$ denote the $i-$th row sum of the matrix T^*. Then

$$\begin{aligned}
\bar{S}_1 &= \bar{F}_i + \bar{G}_i + \bar{H}_i + \bar{I}_i + \bar{J}_i \\
&= -\xi\sigma - \frac{h}{2}\left(3\theta_2 p_{i-1} + \theta_3 p_i - \theta_2 p_{i+1}\right) - h^2\left(\theta_3 s_i + \theta_2 s_{i+1}\right), \\
\bar{S}_i &= \bar{E}_i + \bar{F}_i + \bar{G}_i + \bar{H}_i + \bar{I}_i + \bar{J}_i \\
&= -h^2\left(\theta_2 s_{i-1} + \theta_3 s_i + \theta_2 s_{i+1}\right),\ i = 2(1)N-1, \\
\bar{S}_N &= \bar{E}_i + \bar{F}_i + \bar{G}_i + \bar{C}_i + \bar{H}_i + \bar{I}_i + \bar{J}_i \\
&= -h^2\left(\theta_2 r_{i+1} + \theta_2 s_{i-1} + \theta_3 s_i + \theta_2 s_{i+1}\right), \\
\bar{S}_{N+1} &= \bar{E}_i + \bar{F}_i + \bar{G}_i + \bar{B}_i + \bar{C}_i + \bar{H}_i + \bar{I}_i + \bar{J}_i \\
&= -h^2\left(\theta_3 r_i + \theta_2 r_{i+1} + \theta_2 s_{i-1} + \theta_3 s_i + \theta_2 s_{i+1}\right), \\
\bar{S}_i &= \bar{E}_i + \bar{F}_i + \bar{G}_i + \bar{A}_i + \bar{B}_i + \bar{C}_i + \bar{H}_i + \bar{I}_i + \bar{J}_i \\
&= -h^2\left(\theta_2 r_{i-1} + \theta_3 r_i + \theta_2 r_{i+1} + \theta_2 s_{i-1} + \theta_3 s_i + \theta_2 s_{i+1}\right), \\
\bar{S}_{2N-1} &= \bar{E}_i + \bar{F}_i + \bar{G}_i + \bar{A}_i + \bar{B}_i + \bar{C}_i + \bar{H}_i + \bar{I}_i \\
&= -h^2\left(\theta_2 r_{i-1} + \theta_3 r_i + \theta_2 r_{i+1} + \theta_2 s_{i-1} + \theta_3 s_i\right), \\
\bar{S}_{2N} &= \bar{E}_i + \bar{F}_i + \bar{G}_i + \bar{A}_i + \bar{B}_i + \bar{C}_i + \bar{H}_i \\
&= -h^2\left(\theta_2 r_{i-1} + \theta_3 r_i + \theta_2 r_{i+1} + \theta_2 s_{i-1}\right), \\
\bar{S}_i &= \bar{E}_i + \bar{F}_i + \bar{G}_i + \bar{A}_i + \bar{B}_i + \bar{C}_i \\
&= -h^2\left(\theta_2 r_{i-1} + \theta_3 r_i + \theta_2 r_{i+1}\right),\ i = 2N+1(1)3N-1.
\end{aligned}$$

As we make the calculations progressively more detailed (by letting the mesh size approach zero), a key property of the matrix T^* emerges. It becomes both monotone and irreducible. These properties together guarantee the existence of the inverse of the matrix, with its elements greater than zero. Then

$$\overline{E}_r = T^{*-1}W(h), \tag{12}$$

which implies

$$\|\overline{E}_r\| \leq \|T^{*-1}\|\|W(h)\|. \tag{13}$$

If (j,i)-th element of the inverse matrix of T^* is denoted by $\bar{t}_{j,i}$, then, for $j = 1(1)3N-1$,

$$\sum_{i=1}^{3N-1} \bar{t}_{j,i}\bar{S}_i = 1.$$

So,

$$\sum_{i=1}^{3N-1} \bar{t}_{j,i} \leq \frac{1}{\min_{1\leq i\leq 3N-1} \bar{S}_i} \leq \frac{1}{h^2 \mid \bar{B}_i \mid}. \tag{14}$$

From equations (11), (12), (13) and (14), we have

$$\bar{e}_i = \sum_{j=1}^{3N-1} \bar{t}_{j,i} w_i(h), \quad i = 1(1)3N-1,$$

which implies

$$\begin{aligned} \bar{e}_i &\leq \left(\sum_{j=1}^{3N-1} \overline{v}_{j,i} \right) \max_{1\leq i\leq 3N-1} \mid w_i(h) \mid \\ &\leq \frac{1}{h^2 \mid \bar{B}_{i^*} \mid} \times \frac{h^3 X^*}{2} = O(h), \end{aligned}$$

where X^* is a constant which is independent on h. So $\|\overline{E}_r\| = O(h)$. Hence, our technique is of linear rate of convergence.

4 Numerical Experiments

The schemes (8) give a system of $(3N-1)$ equations in $(3N+1)$ variables, which can be reduced to the system of $(3N-1)$ equations in $(3N-1)$ variables as follows.

$$\bar{F}_i\kappa_i + \bar{G}_i\kappa_{i+1} + \bar{H}_i\kappa_{i-1+N} + \bar{I}_i\kappa_{i+N} + \bar{J}_i\kappa_{i+1+N} = \bar{D}_i - \bar{A}_i u_{i-1-N} - \bar{B}_i u_{i-N} - \bar{C}_i u_{i+1-N} - \bar{E}_i u_{i-1}, \text{ for } i = 1,$$

$$\bar{E}_i\kappa_{i-1} + \bar{F}_i\kappa_i + \bar{G}_i\kappa_{i+1} + \bar{H}_i\kappa_{i-1+N} + \bar{I}_i\kappa_{i+N} + \bar{J}_i\kappa_{i+1+N} = \bar{D}_i - \bar{A}_i u_{i-1-N} - \bar{B}_i u_{i-N} - \bar{C}_i u_{i+1-N}, \text{ for } 2 \leq i \leq N-1,$$

$$\bar{E}_i\kappa_{i-1} + \bar{F}_i\kappa_i + \bar{G}_i\kappa_{i+1} + \bar{C}_i\kappa_1 + \bar{H}_i\kappa_{2N-1} + \bar{I}_i\kappa_{2N} + \bar{J}_i\kappa_{2N+1} = \bar{D}_i - \bar{A}_i u_{-1} - \bar{B}_i u_0, \text{ for } i = N,$$

$$\bar{E}_i\kappa_{i-1} + \bar{F}_i\kappa_i + \bar{G}_i\kappa_{i+1} + \bar{B}_i\kappa_1 + \bar{C}_i\kappa_2 + \bar{H}_i\kappa_{2N} + \bar{I}_i\kappa_{2N+1} + \bar{J}_i\kappa_{2N+2} = \bar{D}_i - \bar{A}_i u_0, \text{ for } i = N+1,$$

$$\bar{E}_i\kappa_{i-1} + \bar{F}_i\kappa_i + \bar{G}_i\kappa_{i+1} + \bar{A}_i\kappa_{i-1-N} + \bar{B}_i\kappa_{i-N} + \bar{C}_i\kappa_{i+1-N} + \bar{H}_i\kappa_{i-1+N} + \bar{I}_i\kappa_{i+N} + \bar{J}_i\kappa_{i+1+N} = \bar{D}_i, \text{ for } N+2 \leq i \leq 2N-2,$$

$$\bar{E}_i\kappa_{i-1} + \bar{F}_i\kappa_i + \bar{G}_i\kappa_{i+1} + \bar{A}_i\kappa_{i-1-N} + \bar{B}_i\kappa_{i-N} + \bar{C}_i\kappa_{i+1-N} + \bar{H}_i\kappa_{i-1+N} + \bar{I}_i\kappa_{i+N} = \bar{D}_i - \bar{J}_i v_{3N}, \text{ for } i = 2N-1,$$

$$\bar{E}_i\kappa_{i-1} + \bar{F}_i\kappa_i + \bar{G}_i\kappa_{i+1} + \bar{A}_i\kappa_{i-1-N} + \bar{B}_i\kappa_{i-N} + \bar{C}_i\kappa_{i+1-N} + \bar{H}_i\kappa_{i-1+N} = \bar{D}_i - \bar{I}_i v_{3N} - \bar{J}_i v_{3N+1}, \text{ for } i = 2N,$$

$$\bar{E}_i\kappa_{i-1} + \bar{F}_i\kappa_i + \bar{G}_i\kappa_{i+1} + \bar{A}_i\kappa_{i-1-N} + \bar{B}_i\kappa_{i-N} + \bar{C}_i\kappa_{i+1-N} = \bar{D}_i - \bar{H}_i v_{i-1+N} - \bar{I}_i v_{i+N} - \bar{J}_i v_{i+1+N}, \text{ for } i = 2N+1 \le i \le 3N-1.$$

We make use of the function $v(x)$ in the interval $[3, 4]$. This is then solved using Gauss elimination method with the help of MATLAB R2022a mathematical software.

We tested our proposed method through two numerical experiments and confirmed it works well. The solution is presented in tables for various levels of perturbation values by changing the level of mesh size in the simulations. A technique called the double-mesh principle is used on these examples to find the maximum absolute errors.

$$E^N = \max_i \mid \kappa_i^N - \kappa_{2i}^{2N} \mid .$$

Rate of Convergence

We employ the double mesh principle to determine the convergence rate, denoted by $\bar{\rho}$ and defined as:

$$\bar{\rho} = \frac{\log(E_h/E_{h/2})}{\log 2}.$$

Example 1. To demonstrate the capabilities of this method, we analyze the following problem:

$$-\xi\kappa''(x) + 5\kappa'(x) + 2\kappa(x) - \kappa(x-1) + \kappa(x+1) = 1, \ x \in \gamma = (0, 3),$$

satisfying

$$\begin{aligned} \kappa(x) &= 1, \ x \in [-1, 0], \\ \kappa(x) &= 2, \ x \in [3, 4]. \end{aligned}$$

This section delves deeper into the results for the first example. Table 1 shows how the solution's accuracy (maximum absolute error) changes as a key parameter (the perturbation parameter denoted by ξ) is varied across different scales (from 10^{-3} to 10^{-10}). The table also considered solutions obtained using different mesh sizes (N values ranging from 16 to 512). For reference, Figure 1(a) visualizes the solution when the perturbation parameter is set to 10^{-4} (one specific data point from Table 1) and Figure 2(a) depicts the point-wise absolute error of this example for varying N values. Going a step further, Table 2 calculates the rate of convergence for this example. By analyzing both Table 2 and the theoretical convergence analysis, we can see that the proposed method converges at a linear rate. In simpler terms, the error reduces proportionally as the mesh size is refined.

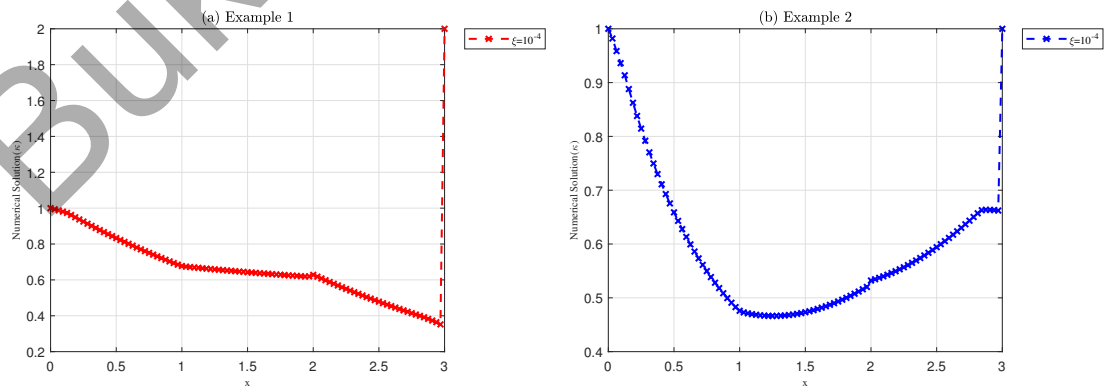

Figure 1. The numerical solution of Example 1 and Example 2 for $\xi = 10^{-4}$

Table 1

The maximum absolute error of Example 1 for different values of ξ

ξ	N					
	16	32	64	128	256	512
10^{-3}	2.1481e-02	1.1610e-02	6.0264e-03	3.0690e-03	1.5485e-03	7.7920e-04
10^{-4}	2.1481e-02	1.1610e-02	6.0264e-03	3.0690e-03	1.5485e-03	7.7775e-04
10^{-5}	2.1481e-02	1.1610e-02	6.0264e-03	3.0690e-03	1.5485e-03	7.7775e-04
10^{-6}	2.1481e-02	1.1610e-02	6.0264e-03	3.0690e-03	1.5485e-03	7.7775e-04
10^{-7}	2.1481e-02	1.1610e-02	6.0264e-03	3.0690e-03	1.5485e-03	7.7775e-04
10^{-8}	2.1481e-02	1.1610e-02	6.0264e-03	3.0690e-03	1.5485e-03	7.7775e-04
10^{-9}	2.1481e-02	1.1610e-02	6.0264e-03	3.0690e-03	1.5485e-03	7.7775e-04
10^{-10}	2.1481e-02	1.1610e-02	6.0264e-03	3.0690e-03	1.5485e-03	7.7775e-04
E^N	2.1481e-02	1.1610e-02	6.0264e-03	3.0690e-03	1.5485e-03	7.7775e-04

Table 2

Rate of convergence of Example 1 for $\xi = 10^{-4}$

	h	$\frac{h}{2}$	E_h	$\frac{h}{4}$	$E_{\frac{h}{2}}$	ρ
	1/16	1/32	2.1481e-02	1/64	1.1610e-02	0.8877
	1/32	1/64	1.1610e-02	1/128	6.0264e-03	0.9460
	1/64	1/128	6.0264e-03	1/256	3.0690e-03	0.9735

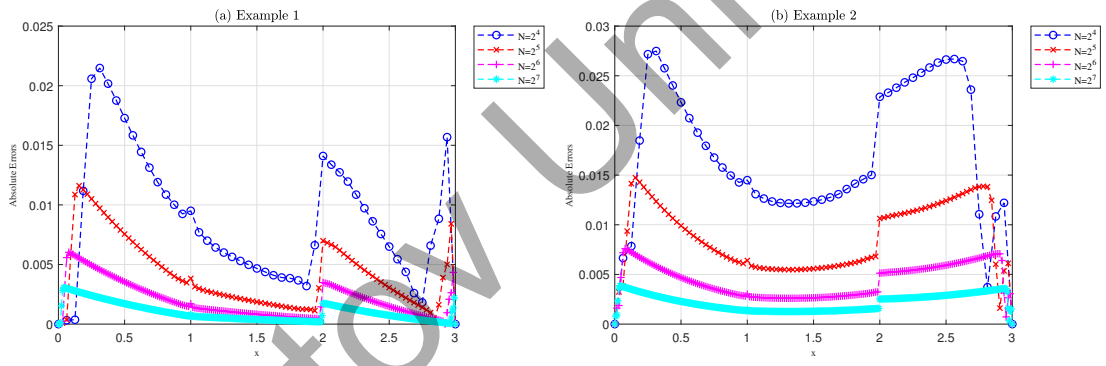

Figure 2. The point-wise absolute errors of Example 1 and Example 2 for different values of N

Example 2. To demonstrate the capabilities of this method, we analyze the following problem:

$$-\xi\kappa''(x) + (x+5)\kappa'(x) + 2\kappa(x) - \kappa(x-1) + x\kappa(x+1) = x, x \in \gamma = (0,3),$$

satisfying

$$\begin{aligned} \kappa(x) &= 1,\ x \in [-1,0], \\ \kappa(x) &= 1,\ x \in [3,4]. \end{aligned}$$

This section delves deeper into the results for the first example. Table 3 shows how the solution's accuracy (maximum absolute error) changes as a key parameter (the perturbation parameter denoted by ξ) is varied across different scales (from 10^{-3} to 10^{-10}). The table also considered solutions obtained using different mesh sizes (N values ranging from 16 to 512). For reference, Figure 1(b) visualizes the solution when the perturbation parameter is set to 10^{-4} (one specific data point from Table 3) and Figure 2(b) depicts the point-wise absolute error of this example for varying N values. Going a step further, Table 4 calculates the rate of convergence for this example. By analyzing both Table 4 and the theoretical convergence analysis, we can see that the proposed method converges at a linear rate. In simpler terms, the error reduces proportionally as the mesh size is refined.

Table 3

The maximum absolute error of Example 2 for different values of ξ

ξ	N					
	16	32	64	128	256	512
10^{-3}	2.7489e-02	1.4740e-02	7.6052e-03	3.8568e-03	1.9394e-03	2.1622e-03
10^{-4}	2.7489e-02	1.4740e-02	7.6052e-03	3.8568e-03	1.9411e-03	9.7360e-03
10^{-5}	2.7489e-02	1.4740e-02	7.6052e-03	3.8568e-03	1.9411e-03	9.7360e-03
10^{-6}	2.7489e-02	1.4740e-02	7.6052e-03	3.8568e-03	1.9411e-03	9.7360e-03
10^{-7}	2.7489e-02	1.4740e-02	7.6052e-03	3.8568e-03	1.9411e-03	9.7360e-03
10^{-8}	2.7489e-02	1.4740e-02	7.6052e-03	3.8568e-03	1.9411e-03	9.7360e-03
10^{-9}	2.7489e-02	1.4740e-02	7.6052e-03	3.8568e-03	1.9411e-03	9.7360e-03
10^{-10}	2.7489e-02	1.4740e-02	7.6052e-03	3.8568e-03	1.9411e-03	9.7360e-03
E^N	2.7489e-02	1.4740e-02	7.6052e-03	3.8568e-03	1.9411e-03	9.7360e-03

Table 4

Rate of convergence of Example 2 for $\xi = 10^{-4}$

	h	$\frac{h}{2}$	E_h	$\frac{h}{4}$	$E_{\frac{h}{2}}$	ρ
	1/16	1/32	2.7489e-02	1/64	1.4740e-02	0.8992
	1/32	1/64	1.4740e-02	1/128	7.6052e-03	0.9546
	1/64	1/128	7.6052e-03	1/256	3.8568e-03	0.9796

Conclusion

This study tackles a specific class of differential equations: singularly perturbed differential difference equations with mixed shifts. These equations involve delays (where the solution depends on a past state) and advances (where it depends on a future state). The authors propose a solution method using non-polynomial splines. This approach is unique because it incorporates a fitting factor, that can be adjusted within different intervals of the problem. To demonstrate the effectiveness of this method, two examples are presented. For each example, corresponding figures (Figure 1 and Figure 2) visualize the numerical solution alongside the point-wise absolute errors. Additionally, tables (Table 1 and Table 3) summarize the maximum absolute errors for each example. These results all point towards convergence of the numerical solution to the true solution. In other words, as the mesh size in the calculations is reduced, the error gets smaller. Interestingly, both theoretical analysis and the numerical results suggest a convergence rate of one (see Tables 2 and 4), which is a desirable property in numerical methods.

Author Contributions

All authors contributed equally to this work.

Conflict of Interest

The authors declare no conflict of interest.

References

1 Debela, H.G., Kejela, S.B., & Negassa A.D. (2020). Exponentially fitted numerical method for singularly perturbed differential-difference equations. *International Journal of Differential Equations, 2020*(1), 5768323. https://doi.org/10.1155/2020/5768323

2 Kiltu, G.G., Duressa, G.F., & Bullo, T.A. (2021). Computational method for singularly perturbed delay differential equations of the reaction-diffusion type with negative shift. *Journal of Ocean Engineering and Science, 6*(3), 285–291. https://doi.org/10.1016/j.joes.2021.02.001

3 Duressa, G.F., & Bullo, T.A. (2021). Higher-order numerical method for singularly perturbed delay reaction-diffusion problems. *Pure and Applied Mathematics, 10*(3), 68–76. https://doi.org/10.11648/j.pamj.20211003.11

4 Vaid, M.K., & Arora, G. (2019). Solution of second order singular perturbed delay differential equation using trigonometric B-spline. *International Journal of Mathematical, Engineering and Management Sciences, 4*(2), 349–360. https://dx.doi.org/10.33889/IJMEMS.2019.4.2-028

5 Tirfesa, B.B., Duressa, G.F., & Debela, H.G. (2022). Non-polynomial cubic spline method for solving singularly perturbed delay reaction-diffusion equations. *Thai Journal of Mathematics, 20*(2), 679–692.

6 Joy, D., & Kumar, S.D. (2024). Computational techniques for singularly perturbed reaction-diffusion delay differential equations: a second-order approach. *Journal of Mathematics and Computer Science, 35*(3), 304–318. https://dx.doi.org/10.22436/jmcs.035.03.04

7 Chakravarthy, P.P., Kumar. S.D., & Rao, R.N. (2017). Numerical solution of second order singularly perturbed delay differential equations via cubic spline in tension. *International Journal of Applied and Computational Mathematics, 3*, 1703–1717. https://doi.org/10.1007/s40819-016-0204-5

8 Srinivas, E., & Phaneendra, K. (2024). A novel numerical scheme for a class of singularly perturbed differential-difference equations with a fixed large delay. *Bulletin of the Karaganda University. Mathematics Series,* 1(113), 194–207. https://doi.org/10.31489/2024m1/194-207

9 Abdulla, M.I., Duressa, G.F., & Debela, H.G. (2021). Robust numerical method for singularly perturbed differential equations with large delay. *Demonstratio Mathematica, 54*(1), 576–589. https://doi.org/10.1515/dema-2021-0020

10 Regal, A.M., & Kumar, D. (2024). Singular perturbations and large time delays through accelerated spline-based compression technique. *Contemporary Mathematics,* 1072–1092. https://doi.org/10.37256/cm.5120244269

11 Ejere, A.H., Duressa, G.F., Woldaregay, M.M., & Dinka, T.G. (2022). An exponentially fitted numerical scheme via domain decomposition for solving singularly perturbed differential equations with large negative shift. *Journal of Mathematics, 2022*(1), 974134. https://doi.org/10.1155/2022/7974134

12 Asha, S., & Paramasivam, M.J. (2022). A novel method for solving type-2 intuitionistic fuzzy transportation problems using singularly perturbed delay differential equations. *Advances and Applications in Mathematical Sciences, 21*(8), 4483–4491.

13 Chakravarthy, P.P., & Kumar, K. (2021). A novel method for singularly perturbed delay differential equations of reaction-diffusion type. *Differential Equations and Dynamical Systems, 29*, 723–734. https://doi.org/10.1007/s12591-017-0399-x

14 Joy, D., & Kumar, S.D. (2024). Non-polynomial spline approach for solving system of singularly perturbed delay differential equations of large delay. *Mathematical and Computer Modelling of Dynamical Systems, 30*(1), 179–201. https://doi.org/10.1080/13873954.2024.2314600

15 Senthilkumar, L.S., Mahendran, R., & Subburayan, V. (2022). A second order convergent initial

value method for singularly perturbed system of differential-difference equations of convection diffusion type. *Journal of Mathematics and Computer Science, 25*(1), 73–83. http://dx.doi.org/10.22436/jmcs.025.01.06

16 Chakravarthy, P.P., & Gupta, T. (2020). Numerical solution of a weakly coupled system of singularly perturbed delay differential equations via cubic spline in tension. *National Academy Science Letters, 43*, 259–262. https://doi.org/10.1007/s40009-019-00806-0

17 Sirisha, L., Phaneendra, K., & Reddy, Y.N. (2018). Mixed finite difference method for singularly perturbed differential difference equations with mixed shifts via domain decomposition. *Ain Shams Engineering Journal, 9*(4), 647–654. https://doi.org/10.1016/j.asej.2016.03.009

18 Swamy, D.K., Singh, R.P., & Reddy, Y.N. (2022). Numerical integration method for a class of singularly perturbed differential-difference equations. *Mathematical Statistician and Engineering Applications, 71*(4), 5771–5795.

19 Ghassabzade, F.A., Saberi-Nadjafi, J., & Soheili, A.R. (2021). A method based on the meshless approach for the numerical solution of the singularly perturbed differential-difference equation arising in the modeling of neuronal variability. *Caspian Journal of Mathematical Sciences, 10*(2), 210–223. https://doi.org/10.22080/CJMS.2020.18475.1474

20 Priyadarshana, S., Sahu, S.R., & Mohapatra, J. (2022). Asymptotic and numerical methods for solving singularly perturbed differential difference equations with mixed shifts. *Iranian Journal of Numerical Analysis and Optimization, 12*(1), 55–72. http://dx.doi.org/10.22067/ijnao.2021.70731.1038

21 Adilaxmi, M., Bhargavi, D., & Reddy, Y.N. (2019). An initial value technique using exponentially fitted non standard finite difference method for singularly perturbed differential-difference equations. *Applications and Applied Mathematics: An International Journal (AAM), 14*(1), 16.

22 Ayalew, M., Kiltu, G.G., & Duressa, G.F. (2021). Fitted numerical scheme for second-order singularly perturbed differential-difference equations with mixed shifts. *In Abstract and Applied Analysis, 2021*, 4573847. https://doi.org/10.1155/2021/4573847

23 Melesse, W.G., Tiruneh, A.A., & Derese, G.A. (2019). Solving linear second-order singularly perturbed differential difference equations via initial value method. *International Journal of Differential Equations, 2019*, 5259130. https://doi.org/10.1155/2019/5259130

Author Information[*]

Akhila Mariya Regal — Master of Philosophy, Research Scholar, Department of Mathematics, School of Advanced Sciences, Vellore Institute of Technology, Vellore, 632014, Tamil Nadu, India; e-mail: *akhilamariyard@gmail.com*; https://orcid.org/0009-0005-3798-3068

S Dinesh Kumar (*corresponding author*) — Doctor of Philosophy, Assistant Professor Senior Grade, Department of Mathematics, School of Advanced Sciences, Vellore Institute of Technology, Vellore, 632014, Tamil Nadu, India; e-mail: *mathdinesh005@gmail.com*; https://orcid.org/0000-0003-4374-9292

[*]The author's name is presented in the order: First, Middle, and Last Names.